Desalination and Water Treatment
www.deswater.com
doi: 10.5004/dwt.2021.26980

218 (2021) 327–344
April

Effective removal of lead ions from wastewater using multi-walled carbon nanotubes functionalized by organophosphonic acid

Zhihua Jia, Ping Yin*, Zhenglong Yang*, Xiguang Liu, Yanbin Xu, Feng Wang, Wenjun Sun, Huawei Yang, Honglan Cai

School of Chemistry and Materials Science, Ludong University, Yantai 264025, China, Tel. +86-535-6696162; Fax: +86-535-6697667; email: yinping426@163.com (P. Yin), Tel. +86-13695352875; email: yzl@iccas.ac.cn (Z. Yang), Tel. +86-17861191558; email: zhihuajia_ldu@163.com (Z. Jia), Tel. +86-13963882897; email: xgliu1986@163.com (X. Liu), Tel. +86-15953542833; email: xuyb_lzu@hotmail.com (Y. Xu), Tel. +86-15053504617; email: Wf200818@126.com (F. Wang), Tel. 86-18953549264; email: sunwenjuan1108@126.com (W. Sun), Tel. +86-15668085255; email: huaweiyang@tju.edu.cn (H. Yang), Tel. +86-15866451889; email: honglancai@163.com (H. Cai)

Received 24 December 2019; accepted 21 December 2020

ABSTRACT

Lead is one of the most common toxic pollutants found in industrial effluents, which can do harm to ecosystem and human health. In the present study, organodiphosphonic acid functionalized multi-walled carbon nanotubes (DPA-MWCNTs) have developed and efficiently been utilized to remove lead ions from wastewater. The relevant adsorption behaviors of DPA-MWCNTs for lead ions, such as the effect of pH, adsorption kinetics, adsorption isotherm, and thermodynamics as well, have also been investigated. The results indicate that the adsorption kinetics of DPA-MWCNTs for lead ions at different temperatures can be modeled by the pseudo second-order rate equation, the experimental data fit well with the Langmuir isotherm model, which indicates the monolayered way of the adsorption and the maximum adsorption capacities of DPA-MWCNTs for lead ions could reach 757.58 mg/g, which is much higher than that of other adsorbents reported in the literatures, and the excellent features of DPA-MWCNTs for lead ions removal can ensure their applicability and feasibility in the industrial scale. The evaluation of adsorption thermodynamic parameters ($\Delta G°$, $\Delta H°$, and $\Delta S°$) suggests the spontaneous and endothermic nature of the adsorption process with the increase of the randomness. Moreover, the adsorption process optimization is performed using response surface methodology (RSM), and the analysis of variance (ANOVA) of the quadratic model demonstrated that the model is highly significant. From the obtained results, it has been found that DPA-MWCNTs can be used as a kind of adsorbent with high efficiency in wastewater treatment and water purification, which would provide a facile processing for lead removal.

Keywords: Adsorption; Lead ion removal; DPA-MWCNTs; Functionalization

1. Introduction

Lead, one of the toxic elements, has non-biodegradable behavior, bio-accumulative nature, and has been recognized to pose severe risks to human health and the environment. Its release in nature could lead to soil and underground contamination, and even low dosage of lead can cause serious negative effects and diseases, which could affect the lungs, kidneys, and nervous systems, especially those of children. Therefore, its presence in the aquatic environment is a major concern, and the attention to the development of technologies of eliminating lead pollution in the whole world is growing rapidly [1]. Several methods have been

* Corresponding authors.

introduced for lead removal from contaminated water to make the water safe and suitable for consumption, and the widely used methods of lead removal include adsorption, oxidation, precipitation, electrochemical method, coagulation, floating, ion exchange, membrane separation and so on. Among these methods to treat contaminated wastewaters, adsorption is the most effective, economic, efficient, and simplest. It is superior to other conventional methods due to its high level of effectiveness in removing lead ions from industrial wastewater, the simple and amenable process, the ready availability of absorbents, and the striking recyclability [2–5].

Nowadays, there is a strong research interest in developing the adsorbents that have high efficiency and selectivity, and a wide range of adsorbents have been used for lead adsorption. Efficient adsorbents have become the decisive factor in lead removal processes, and many different types of adsorbents have been developed and used in order to obtain good removal performances, for example, poly(aniline-co-pyrrole) nanospheres [6], 5-sulfosalicyclic acid modified lignin [7], biochar [1,8], fly ash [9], PVA/PAA nanofibers [10], magnetite-modified with Schiff bases [11], graphene oxide-MgO nanohybrid [12], etc. To further improve adsorption efficiency, the discovery of application of more efficient adsorbents becomes necessary. Carbon nanotubes have striking unique chemical and physical properties such as excellent mechanical properties and thermal stability, high specific surface area, tunable surface chemistry, and non-corrosive property, which have emerged to be excellent heavy metal ion adsorbents [13,14]. However, the adsorption of metal ions by raw CNTs can be inhibited because of the strong van der Waals interactions between the raw CNTs and metals, which lead to difficult dispersion of CNTs in solvents. Introducing other functional groups in CNTs could improve the hydrophilicity and provide coordination atoms that are able to facilitate the separation and removal of heavy metal ions from water solutions. Especially when some types of functional groups are chemically modified onto their surface, the chemical functionalization could remarkably improve their adsorption capacity and adsorption selectivity to heavy metal ions since the removal of metal ions by CNTs adsorption is usually dominated by the surface complexation [15]. There are various organophosphonic acids with diverse structures, and the presence of oxygen atoms in $–PO_3$ groups in organophosphonic acids can enable them to coordinate with metal ions. Diphosphonic acid (DPA, hydroxyethylidenediphosphonic acid) can be a candidate for coordinating with metal ions, where the organic part plays the role of a controllable spacer, hydroxyl group and three $–PO_3$ groups can coordinate with metal ions. If these functional organophosphonic acid groups are grafted on a solid matrix, the chemical modification would overcome their shortcoming of being soluble in water and allow them to be used in the adsorption of metal ions from aqueous solutions.

The aim of this paper is to explore a simple and effective method to improve the adsorption ability of carbon nanotubes, and hydroxyethylidenediphosphonic acid containing hydroxyl and phosphonic acid groups has been introduced to the surface of multi-walled carbon nanotubes via facile esterification reaction. The diphosphonic acid functional groups introduced onto the surface of DPA-MWCNTs, which could chelate effectively with lead ions and therefore efficiently promote its adsorption properties. So far, there are no papers on organodiphosphonic acid-modified carbon nanotubes adsorption materials for lead ions removal. DPA-MWCNTs with excellent lead ions adsorption properties in our present work is a novel adsorbent for lead ions, which could provide a facile process for lead removal, and have a great potential application. The adsorption performance of DPA-MWCNTs for lead ions from stimulated wastewater has been evaluated using batch experiment, which includes kinetic, isotherm, and thermodynamic modeling of adsorption. Furthermore, RSM has been employed to optimize the relevant adsorption process parameters, and it is also possible to observe the effects of individual variables and their combinations of interactions on the response by using RSM.

2. Experimental details

2.1. Materials and instruments.

2.5 g of the hydroxylated MWCNTs are washed with distilled water and sonicated for 10 min, then oxidized by a 3:1 sulfuric acid and nitric acid mixture. After the refluxing process for 4 h, the mixture is filtered and washed until pH of the filtrate is close to 6, and then dried at 60°C. 20 mL of 50% HEDP(hydroxyethylidenediphosphonic acid) has been mixed with 5.0 g of above-mentioned treated MWCNTs, and they react at temperature of 120°C for 4 h, after that, the samples are washed with deionized water until pH (the filtrate) ≈ 6 and dried at 60°C, which is labeled as DPA-MWCNTs. Simulated wastewater with different concentrations of lead ions has been prepared, and the pH of solution is adjusted using NaOH and HCl. The hydroxylated MWCNTs are chemically pure grade, which have been provided by Chinese Academy of Sciences Chengdu Organic Chemistry Co., Ltd. (China), and all other reagents used in the experiments are analytical grade and purchased from Sinopharm Chemical Reagent Co. Ltd. (China), which are used without any further purification, and all solutions have been prepared with deionized water.

The X-ray diffraction (XRD) patterns from 5.0° to 70.0° have been recorded with a Rigaku Max-2500VPC diffractometer using Cu-Ka_1 radiation. Infrared spectra (FT-IR) of samples are reported in the range of 4,000–400 cm^{-1} with a resolution of 4 cm^{-1}, by accumulating 32 scans using a Nicolet (USA) MAGNA-IR 550 (series II) spectrophotometer. Thermogravimetric (TG) analysis is recorded on a Netzsch STA 409 (Germany), Test conditions: type of crucible, DTA/TG crucible Al_2O_3; nitrogen atmosphere, flow rate 30 mL/min; heating rate: 10 K/min. The XPS (X-ray photoelectron spectroscopy) measurement is made on a PerkinElmer PHI 550-ESCA/SAM (USA) photoelectron spectrometer operated at 10 kV and 30 mA. High resolution XPS spectra are generated with the analyzer pass energy setting at 10 and 50 eV, respectively. The scanning electron microscopy (SEM) and the energy-dispersive X-ray (EDX) of the samples are performed on a HITACHI SU8010 analytical instrument (Japan). Porous structure parameters were characterized using an automatic physisorption analyzer ASAP 2020 (Micromeritics Instruments Corporation, USA) by Brunauer–Emmett–Teller

(BET) and Barret–Joynet–Halenda (BJH) methods through N_2 adsorption at 77 K. Atomic absorption analysis of transition metal ions is performed with a flame atomic absorption GBC-932A spectrophotometer (GBC Co., Australia).

2.2. Effect of pH on adsorption

The effect of pH on the adsorption of lead ions has been studied by adding 20.0 mg of DPA-MWCNTs to 2.0 mmol/L Pb(II) at different pH values (2.0–6.0) in 100 mL Erlenmeyer flask. The mixture was equilibrated for 24 h on a thermostat-cum-shaking assembly at 25°C. Then the solutions are separated from the adsorbents and the concentration of lead ions is detected by atomic absorption spectrometer.

The adsorption amount can be calculated according to Eq. (1):

$$q = \frac{\left(C_0 - C_e\right)V}{W} \tag{1}$$

where q is the adsorption amount (mg/g); C_0 and C_e are the initial and equilibrium concentrations of lead ions (mg/mL) in solution, respectively; V is the volume of the solution (mL); W is the weight of DPA-MWCNTs (g).

2.3. Adsorption kinetics

The adsorption kinetics on the uptake of lead ions by the adsorbent has been studied by placing 20.0 mg of DPA-MWCNTs with 10 mL of lead ion solution in a series of flasks at pH = 5.5 and 5°C–35°C with the concentration of lead ions being 2.0 mmol/L. At a certain time interval, the adsorbent is filtrated and the concentrations of lead ions in solutions are measured.

2.4. Adsorption isotherms

The isotherm adsorption property of the adsorbents is also investigated by batch tests. The adsorption isotherms can be studied using 20.0 mg of DPA-MWCNTs with different lead ions concentrations (1.0–5.0 mmol/L, 10–100 mg/L) at pH 5.5 and 15°C–35°C for 24 h.

2.5. Desorption and recycling studies

To investigate the desorption properties of the adsorbed lead ions from DPA-MWCNTs, the relative experiments have been conducted as follows: After the adsorption process, the lead ion-loaded adsorbents are separated and washed with deionized water to remove unadsorbed lead ions on the surface of DPA-MWCNTs. Then, they are resuspended and stirred in the different solutions of 0.1 mmol/L nitric acid, 0.1 mmol/L nitric acid + 1.0% thiourea, 0.1 mmol/L nitric acid + 2.0% thiourea, 0.1 mmol/L nitric acid + 3.0% thiourea, 0.1 mmol/L nitric acid + 4.0% thiourea, and 0.1 mmol/L nitric acid + 5.0% thiourea, respectively, which are employed as the desorption medium, at 25°C for 24 h to remove the adsorbed lead ions. The desorbed lead ions are separated from DPA-MWCNTs by centrifugal separation and are detected using AAS. The recovered DPA-MWCNTs are thoroughly washed with deionized water and absolute ethanol, dried at 60°C, and then employed in the further adsorption studies. The desorption ratio of lead ions can be calculated as the ratio of the amount of desorbed lead ions to the amount of initially absorbed lead ions. The lead ions adsorption efficiency has been evaluated after each adsorption–desorption cycle, and these processes have been repeated to further ascertain the recycling property of DPA-MWCNTs.

2.6. Experimental design and optimization

The optimization of adsorption conditions is obtained using response surface methodologies (RSM). In this work, the central composite design (CCD) experiment has been introduced, and a Box–Behnken center-united design is employed to design the experiments. The maximum adsorption capacity q has been taken as the responses of the design experiment. Statistical analysis of the model was performed to evaluate the analysis of variance (ANOVA). In order to search for the optimum adsorption conditions for q, the experiments have been conducted according to the CCD experimental plan. With respect to the response surface methodology, a polynomial function containing quadratic terms has been utilized in order to fit an empirical model to the experimental results obtained in relation to the experimental design of CCD, in order to predict the optimum value and subsequently to elucidate the interaction between the factors. The quadratic equation model for predicting the optimal point is presented in Eq. (2):

$$Y = \lambda_0 + \sum_{i=1}^{4}\lambda_i x_i + \sum_{i=1}^{4}\lambda_{ii} x_i^2 + \sum_{i=1}^{3}\sum_{j=i+1}^{4}\lambda_{ij} x_i x_j \tag{2}$$

where λ_0, λ_i, λ_{ii} and λ_{ij} are regression coefficients (λ_0 is constant term, λ_i is linear effect term, λ_{ii} is squared effect term, and λ_{ij} is interaction effect term), and Y is the predicted response value. The optimum values of the selected variables have been obtained by solving the regression equation using Matlab 6.5 software (Math-Works Inc. USA).

3. Results and discussion

3.1. Characterization of DPA-MWCNTs

MWCNTs consist of a group of graphene sheets wrapped around themselves to form cylinders nested together. The surface of the hydroxylated MWCNTs contains a large number of hydroxyl functional groups that are able to react with diphosphonic acid HEDP under the experimental conditions mentioned above (Fig. 1a). The introduction of the diphosphonic acid functional groups onto MWCNTs has very strong coordinating properties and they can chelate with lead ions, and thereby enhance greatly adsorption properties of the adsorbent. Fig. 1b represents XRD patterns of MWCNTs and DPA-MWCNTs, the diffraction peaks observed for all these three samples at $2\theta = 26.0°$ are corresponded to carbon structure, and there is no new diffraction peak appeared after the facile preparation reaction processes. This indicates that the crystal structure of MWCNTs has not been affected by

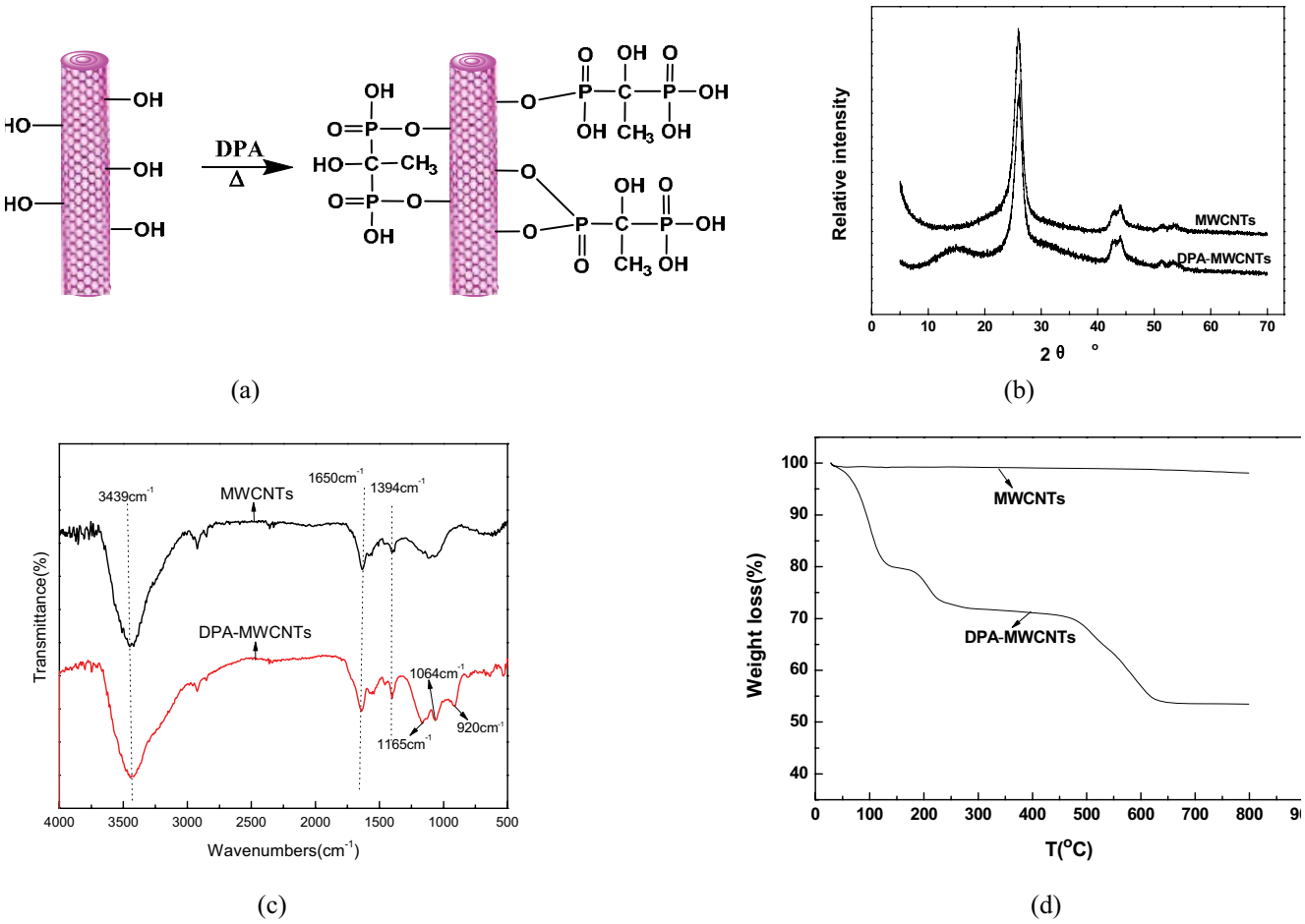

Fig. 1. Synthesis scheme of DPA-MWCNTs (a), XRD patterns of MWCNTs and DPA-MWCNTs (b), FT-IR spectra of MWCNTs and DPA-MWCNTs (c), thermogravimetric curves of MWCNTs and DPA-MWCNTs (d).

the addition of organodiphosphonic acid functional groups, and there is not any essential structure changes occurred after the chemical modification reaction of MWCNTs with hydroxyethylidenediphosphonic acid. Furthermore, it implies that MWCNTs are stable enough to go through the chemical modification reactions, and the organodiphosphonic acid chemical treatment does not change the structure of MWCNTs. FT-IR spectra of MWCNTs and DPA-MWCNTs are shown in Fig. 1c, which could be used to identify the chemical grafting of diphosphonic acids on MWCNTS. In Fig. 1c, comparing with the FT-IR spectrum of MWCNTs, the stretching vibration peaks of PO–(C) located at 910 and 1,064 cm^{-1} and the adsorption peak of P=O at 1,165 cm^{-1} are detected in the spectrum of DPA-MWCNTs, which indicates the presence of PO–(C) and P=O, and that the phosphonic acid groups have been successfully grafted onto MWCNTs [16,17]. Furthermore, the thermogravimetric (TG) curve could reflect the thermal stability of the adsorbent materials. The thermal stability of DPA-MWCNTs is probed by thermal analysis, and TG analysis could also be used to quantify the percentage of functional groups presented on the MWCNTs. The responding results are presented in Fig. 1d, it shows that the weight loss of 12.24% in the temperature range of 25°C–100°C corresponds to the release of physically adsorbed water in DPA-MWCNTs. Further weight loss above 120°C can be attributed to the decomposition of the organic functional groups. The weight loss of 1.14 and 54.93 wt.% between 120°C and 800°C for MWCNTs and DPA-MWCNTs, respectively. Compared with MWCNTs, the additional weight loss of 52.79% is attributed to the presence of diphosphonic acid on the surface of MWCNTs. It is noted that there is just a little weight loss for both DPA-MWCNTs in the temperature range of 25°C–50°C, and the adsorbents usually are utilized below 50°C, hence, DPA-MWCNTs have good thermal stability and it should be applied below 50°C, and it is expected that DPA-MWCNTs can display excellent chemical and physical characteristics to adsorb lead ions due to the introduction of organophosphonic acid chelating functional groups.

Further efforts are required to confirm the chemical modification of organophosphonic acids on the surface of MWCNTs, therefore the X-ray photoelectron spectroscopy (XPS) has been performed on DPA-MWCNTs (Fig. 2). An overview investigation of the peaks in the XPS spectrum of DPA-MWCNTs (Fig. 2a) indicates the presence of carbon, oxygen, and phosphorus. Further analysis of the individual carbon peaks by high resolution XPS (Fig. 2b) reveals that the C1s peak constituted 80.29% (atomic concentration) of

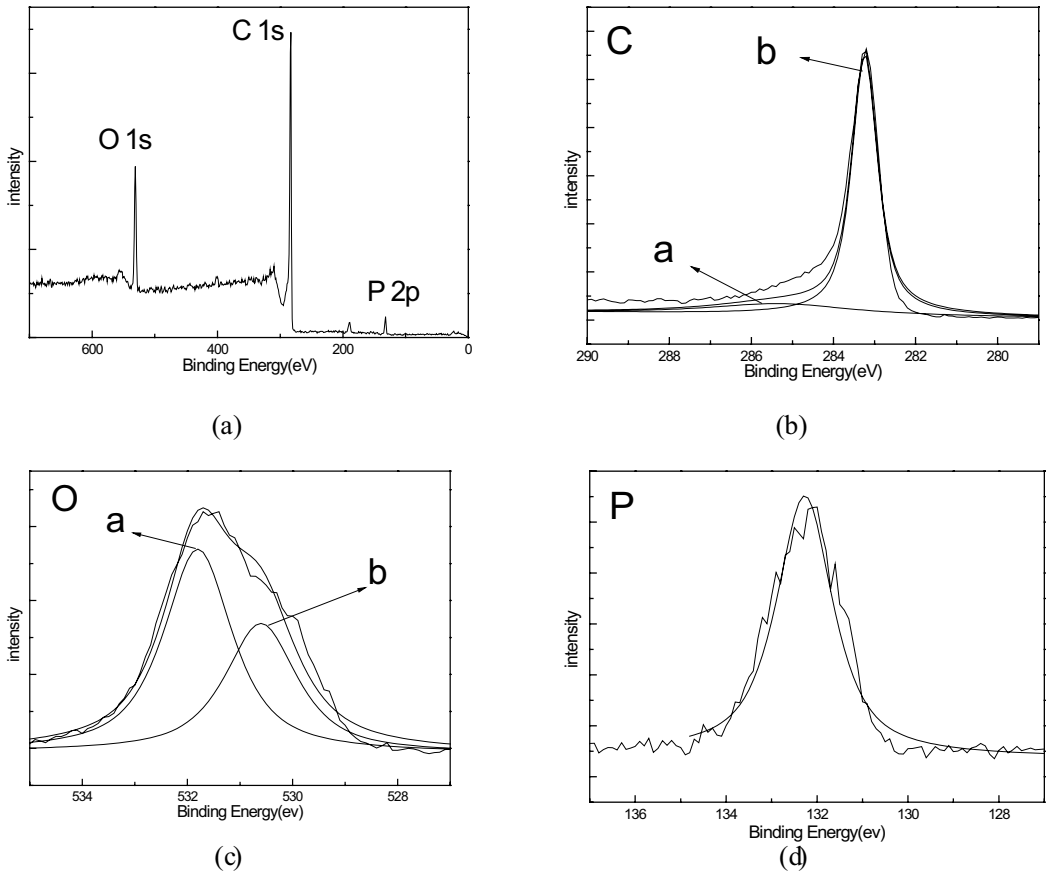

Fig. 2. XPS spectra of DPA-MWCNTs. (a) full survey scan spectrum, (b) C 1s, (c) O 1s, and (d) P 2p.

the sample. The fitted Peak a at 283.24 eV and Peak b at 285.30 eV can be attributed to C–C bond from the carbon nanotube skeleton and carbide, respectively [16]. As seen in Fig. 2c, the individual oxygen peaks by high resolution XPS spectrum, the fitted Peak a at 531.8 eV and Peak b at 530.6 eV belong to P–O, and C=O/P=O. Moreover, that of the individual phosphorus peaks by high resolution XPS (Fig. 2d) shows that the P 2p peak at 132.22 eV constitutes 3.08% of atomic concentration, which can be assigned to phosphorus from P–(C,O) of the phosphonate groups on the DPA-MWCNTs, which is in good agreement with the results of the above-mentioned FT-IR analysis. Therefore, both FT-IR and XPS characterization results have confirmed the presence of the phosphonic acid functional groups in DPA-MWCNTs, and the successful incorporation of the organodiphosphonate functional groups onto the MWCNTs. Saturated adsorption capacities for heavy metal ions are essential parameters for evaluating the adsorption ability of the adsorbents, and the experiments have been carried out with shaking 20.0 mg of the prepared DPA-MWCNTs with 20 mL of metal ion solutions, the mixture is equilibrated at 25°C for 24 h. The static adsorption capacities of DPA-MWCNT for Au(III), Cu(II), Pb(II), Ni(II), Co(II), Zn(II), Cr(III) and Cd(II) ions are 87.12, 14.61, 764.42, 764.42, 19.47, 13.04, 41.92, 26.63, and 5.83 mg/g, respectively, and it is obvious that DPA-MWCNTs have excellent adsorption capacity for Pb(II). DPA-MWCNTs have shown high affinity towards Pb(II), which indicates that the organodiphosphonic acid functional groups existing on the surface of MWCNTs have significant influence on the adsorption properties and can strongly affect and improve the lead ions adsorption capacities in the aqueous solutions. The surface modification is able to further provide binding sites and greatly promote the adsorption properties for some particular metal ions, especially for Pb(II).

3.2. pH effect on the adsorption

The pH of solution, which can affect the existent state of metal ions, the dissociation of functional groups and surface charges in the solution, is a significant parameter in controlling the adsorption process of the metal ions and affecting the adsorption capabilities of metal ions on adsorbents [14]. The relative adsorption experiments at 25°C in the pH range of 2.0–6.0 are conducted in order to evaluate the effect of pH on the adsorption for Pb(II) onto DPA-MWCNTs and optimize the specific pH value for the maximum adsorption efficiency, and the results have been illustrated in Fig. 3. This study of pH effect can help us identify the optimum pH for effective removal. As depicted in this figure, it is clear that in the overall trend, the adsorption capacities increase with the increase of the solution pH values in the pH range of 2.0–5.5. When

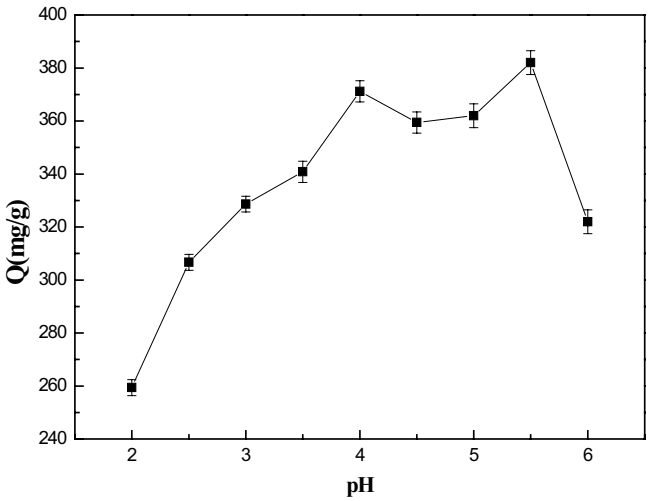

Fig. 3. Effect of pH on the adsorption for Pb(II) on DPA-MWCNTs.

the pH is low, the content of H^+ is high. The lower adsorption capacities of lead ions at lower pH might be attributed to the partial protonation of the active sites, such as O donor atoms of ≡P=O and O–H on the surface of the adsorbent, and the competitive coordination effect of the H^+ ions with lead ions for the adsorption sites of DPA-MWCNTs. Under such more acidic conditions, H^+ ions characteristically have high mobility, the chelation between lead ions and the adsorbent is weak, the surface of the adsorbent DPA-MWCNTs is positively charged, therefore, it is unfavorable for adsorption process because of the electrostatic repulsion towards positively charged lead ions. After that, with the increase of pH, the protonation could weakened, hence the adsorption capacities increase and finally reach the top at pH 5.5. When pH > 5.5, the content of OH^- in the solution increases, it is easy to form the precipitate of $Pb(OH)_2$, therefore, the subsequent lead adsorption kinetics and thermal experiments have been performed at pH 5.5, which is similar to that of the reference [10].

3.3. Adsorption kinetics and determination of the thermodynamics parameters

The adsorption kinetics studies are very crucial in the adsorption process because it affects the design of the lead ions removal treatment plant, which include controlling the experimental conditions that affect the adsorption speed in its race towards equilibrium. From a practical point of view, the rapid kinetics will facilitate smaller reactor volumes ensuring efficiency and economy. To investigate the effect of contact time and temperature on the uptake capacity, the adsorption studies have been carried out by varying the contact time between 0 and 360 min at three different temperatures, that is, 15°C, 25°C, and 3°C. Fig. 4a shows the adsorption kinetics plot of adsorption capacity vs. contact time, which could determine the adsorption equilibrium time. It depicts that the adsorption capacities of DPA-MWCTNs for Pb(II) increases rapidly in the first 25 min of short contact time, and then slow down gradually when approaching equilibrium, and the adsorption process needs at least 6 h to reach the adsorption equilibrium. The kinetic curve is smooth and continuous, leading to saturation, suggesting the possibility of the formation of monolayer coverage of metal ions on the surface of the adsorbent [18]. The reason perhaps is that in the initial fast adsorption step, lead ions might enter easily the accessible pore sites and bind with the phosphonic acid and hydroxyl chelating ligands. While in the slow adsorption step, some lead ions might be hampered to diffusion into the deeper pores. Moreover, it is obvious that with the rise of temperature, the equilibrium adsorption capacity for lead ions increases significantly from 406.8 mg/g (15°C) to 558.6 mg/g (35°C), and the rise of the temperature has provided a greater driving force for the mass transfer and subsequent surface adsorption. These adsorption kinetic studies have revealed the rate of Pb(II) adsorption on the DPA-MWCNTs, moreover, it could provide the necessary information for modeling and designing of the adsorption process. The adsorption procedure of adsorbents for metal ions is generally considered to take place through two mechanisms of film diffusion and particle diffusion. The kinetics experimental results are usually analyzed by Boyd equation and Reichenberg equation in order to distinguish film diffusion from particle diffusion controlled adsorption [19,20]. The relevant equations have been given as follows:

$$F = 1 - \frac{6}{\pi^2}\sum_{n-1}^{\infty}\frac{1}{n^2}\left[\frac{-D_i t\pi^2 n^2}{r_0^2}\right] \tag{3}$$

Or

$$F = 1 - \frac{6}{\pi^2}\sum_{n-1}^{\infty}\frac{1}{n^2}\exp\left[-n^2 Bt\right] \tag{4}$$

and

$$B = \frac{\pi^2 D_i}{r_0^2} = \text{time constant} \tag{5}$$

where n is an integer that defines the infinite series solution; D_i is the effective diffusion coefficient of metal ions in the adsorbent phase; r_0 is the radius of the adsorbent particle, assumed to be spherical; F is the fractional attainment of equilibrium at time t, and it is obtained by the expression:

$$F = \frac{q_t}{q_0} \tag{6}$$

where q_t is the amount of adsorbate taken up at time t and q_0 is the maximum equilibrium uptake. Values of Bt can be obtained from corresponding values of F, and the plots of Bt vs. time t of lead ions onto DPA-MWCNTs at 15°C–35°C are displayed in Fig. 4b, which could be used to distinguish between the film diffusion and particle diffusion controlled adsorption. If the plots were straight line passing through the origin, the adsorption process is dominated by the particle diffusion mechanism, otherwise, it might be governed by the film diffusion. In the present research results, the

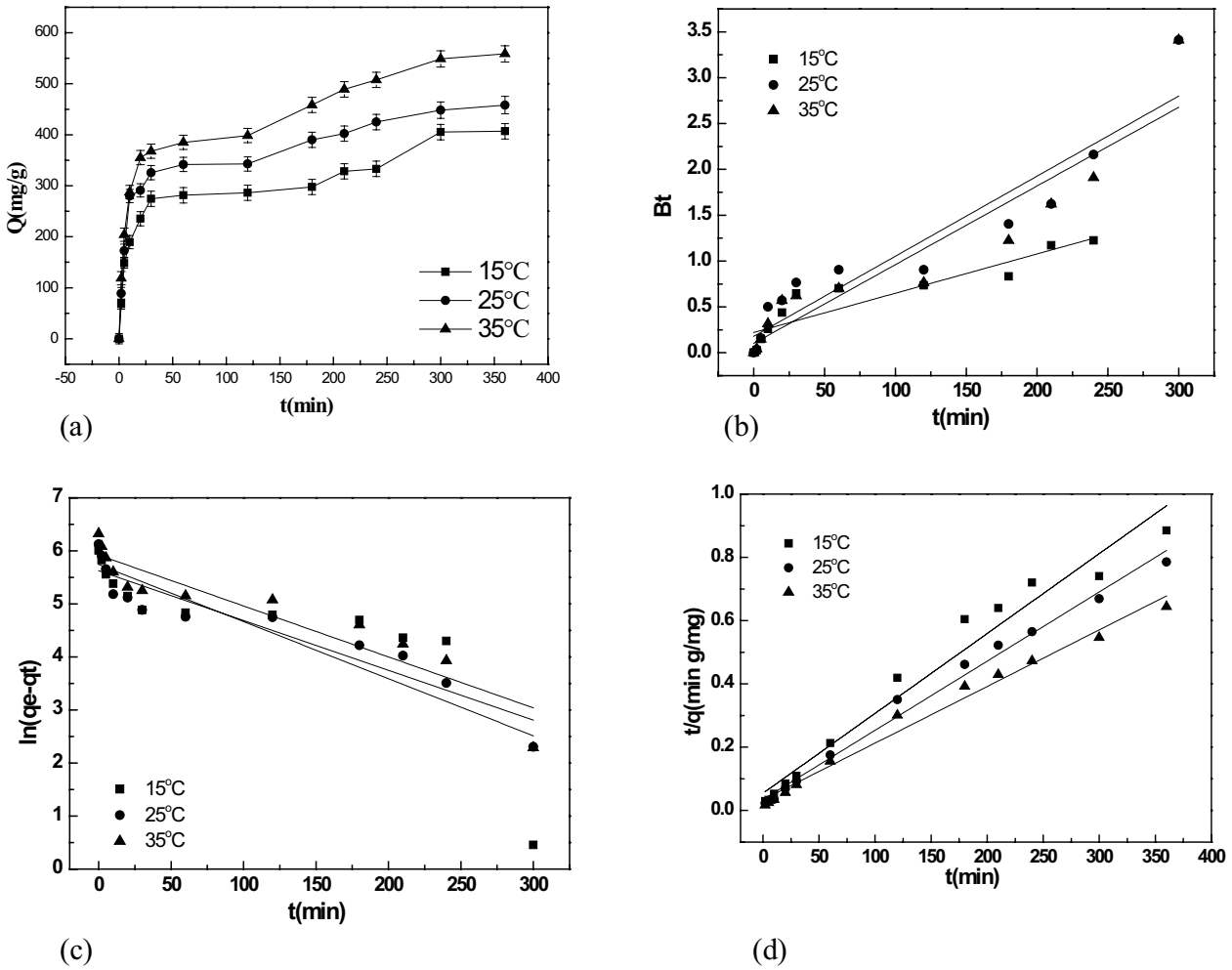

Fig. 4. Kinetic adsorption of Pb(II) onto DPA-MWCNTs at different solution temperatures (a), *Bt* vs. time plots at different solution temperatures of Pb(II) on DPA-MWCNTs (b), the pseudo-first-order kinetic model of DPA-MWCNTs for Pb(II) at various temperatures (c), the pseudo-second-order kinetic plots for the adsorption of Pb(II) on DPA-MWCNTs at various temperatures (d).

lines of *Bt* vs. time plots have not passed through the origin, which indicates the film diffusion, not the particle diffusion, dominates the adsorption processes of DPA-MWCNTs for lead ions.

Furthermore, both the pseudo-first-order equation and the pseudo-second-order equation have been utilized to express the adsorption process of DPA-MWCNTs for lead ions, and they can be expressed by Eqs. (7) and (8) [19,20], respectively:

$$\ln\left(q_e - q_t\right) = \ln q_e - k_1 t \tag{7}$$

$$\frac{t}{q_t} = \frac{1}{k_2 q_e^2} + \frac{t}{q_e} \tag{8}$$

where q_e is the amount of metal adsorbed at equilibrium per unit weight of adsorbent, mg/g, q_t is the amount of metal ion adsorbed at t time, k_1 (min^{-1}) and k_2 (g/mg min) are the rate constants of pseudo-first-order and pseudo-second-order adsorption. The experimental data have been applied to these two kinetics model, and the experimental and calculated q_e values, k_1, k_2 and regression coefficient (R^2) values are presented in Table 1. The pseudo-first-order kinetic and pseudo-second-order kinetic plots for the adsorption of lead ions onto DPA-MWCNTs at different temperatures are shown in Figs. 4c and d, respectively. As seen from Table 1, the obtained coefficients values of the pseudo-second-order model (>0.9672) are better than those of the pseudo-first-order model for the adsorbent (0.6186–0.8764), suggesting the pseudo-second-order model is more suitable to describe the adsorption kinetics of DPA-MWCNTs for lead ions, and the difference between the experimental and calculated value of q_e suggested the suitability of the pseudo-second-order kinetic model. Fig. 4d represents the plots of t/q_t vs. t, which maintain the considerable linearity at all the mentioned temperatures. Therefore, the adsorption kinetics could well be approximated more favorably by pseudo-second-order kinetic model for lead ions onto DPA-MWCNTs.

Table 1
The kinetic parameters of the adsorption for Pb(II) on DPA-MWCNTs at various temperatures

Adsorbent	T (°C)	q_e(exp) (mg/g)	Pseudo-first-order kinetics			Pseudo-second-order kinetics		
			K_1 (min^{-1})	q_e(cal) (mg/g)	R_1^2	$K_2\times 10^{-3}$ (g/mg min)	q_e(cal) (mg/g)	R_2^2
DPA-MWCNTs	15	406.80	0.0108	311.68	0.6186	0.1168	396.83	0.9672
	25	458.26	0.0094	277.13	0.8764	0.1381	456.62	0.9899
	35	558.60	0.0096	373.11	0.8656	0.0948	558.66	0.9851

From the kinetics adsorption experiments, the thermodynamic parameters such as ΔG, ΔH and ΔS, which are necessary for practical application of a process, can be evaluated from the following equations [19,20]:

$$K_c = \frac{C_{Ae}}{C_e} \tag{9}$$

$$\log K_c = \frac{\Delta S}{2.303R} - \frac{\Delta H}{2.303RT} \tag{10}$$

$$\Delta G = -RT\ln K_c \tag{11}$$

where C_e and C_{Ae} are the equilibrium concentration in solution (mg/L) and the solid phase concentration at equilibrium(mg/L), respectively. K_c is the partition coefficients of each temperature. R is the gas constant (8.314 J/mol K), and T is the temperature in Kelvin. The free energy, the enthalpy and the entropy of adsorption of DPA-MWCNTs for lead ions have also been determined, which are important parameters for the design of any industrial adsorption system. From the slope and y-intercept of the linear plot of lnK_c vs. 1/T, the changes of enthalpy and entropy could be obtained. The thermodynamic parameters are listed in Table 2. The positive values of ΔH (48.33 kJ mol^{-1}) indicated that lead ions adsorption on DPA-MWCNTs is endothermic. This result is consistent with the above-mentioned result that the adsorption capacities of lead ions increase with the increasing of temperature. Moreover, DH value can also be used to distinguish what kind of adsorption the process can be classified into. Because the corresponding value (48.33 kJ mol^{-1}) is in the range of 20–80 kJ mol^{-1}, it is indicated that physisorption-chemisorption process might be dominant in the present work. The negative values of ΔG for Pb(II) adsorption on DPA-MWCNTs indicate that the adsorption process is spontaneous, and show the feasibility and thermodynamic spontaneity of this adsorption system, moreover, this feasibility increase with the increase in temperature as can be seen by the more negative value of ΔG at the higher temperature. The positive values of ΔS (172.02 J K^{-1} mol^{-1}) suggest an increase in the randomness at the solid/solution interface during the adsorption process, which is because of the redistribution of energy between the adsorbate lead ions and the adsorbent DPA-MWCNTs.

3.4. Adsorption isotherm

The bonding between soft acids and bases seems to be primarily covalent in nature, thus a strong interaction occurs between large metal ions with high electronegativity (for example, Pt, Au and Pb) and the most polarizable bases. In general, functional groups containing S and N donor atom interact strongly with soft acids like precious metals. Oxygen is a hard base while lead is a soft acid according to HSAB, therefore there are seldom researches on the interaction between these two elements. The significance of this paper is organodiphosphonic acid-modified carbon nanotubes adsorption materials DPA-MWCNTs have been successfully developed, and they have very high adsorption capacity for Pb(II). The adsorption isotherm has been studied in order to explore the relationship between equilibrium adsorption capacity and equilibrium concentration at a certain temperature. The study of adsorption isotherm is very vital and necessary to understand the interactions between adsorbate and adsorbent, and to establish an appropriate correlation of adsorption equilibria in order to optimize the adsorption system. In the present work, it can be found in Fig. 5a that the absorption capacities of lead ions onto DPA-MWCNTs increase along with the increase of temperature. At a certain temperature, the adsorption capacities of lead ions on the adsorbent rises with the increase of the equilibrium concentration. The above-mentioned research results show that this novel organophosphonic acid functionalized carbon nanotubes is very favorable and useful for the lead adsorption, and the high adsorption capacity make it a good promising candidate for lead removal.

The adsorption isotherms were studied and the data are analyzed with Langmuir Eq. (12) and Freundlich Eq. (3)

Table 2
Adsorption thermodynamic parameters of DPA-MWCNTs for Pb(II)

Adsorbent	T (K)	ΔG (kJ/mol)	ΔH (kJ/mol)	ΔS (J/K mol)
DPA-MWCNTs	288	–1,473.02	48.33	172.02
	298	–2,386.33		
	308	–4,949.78		

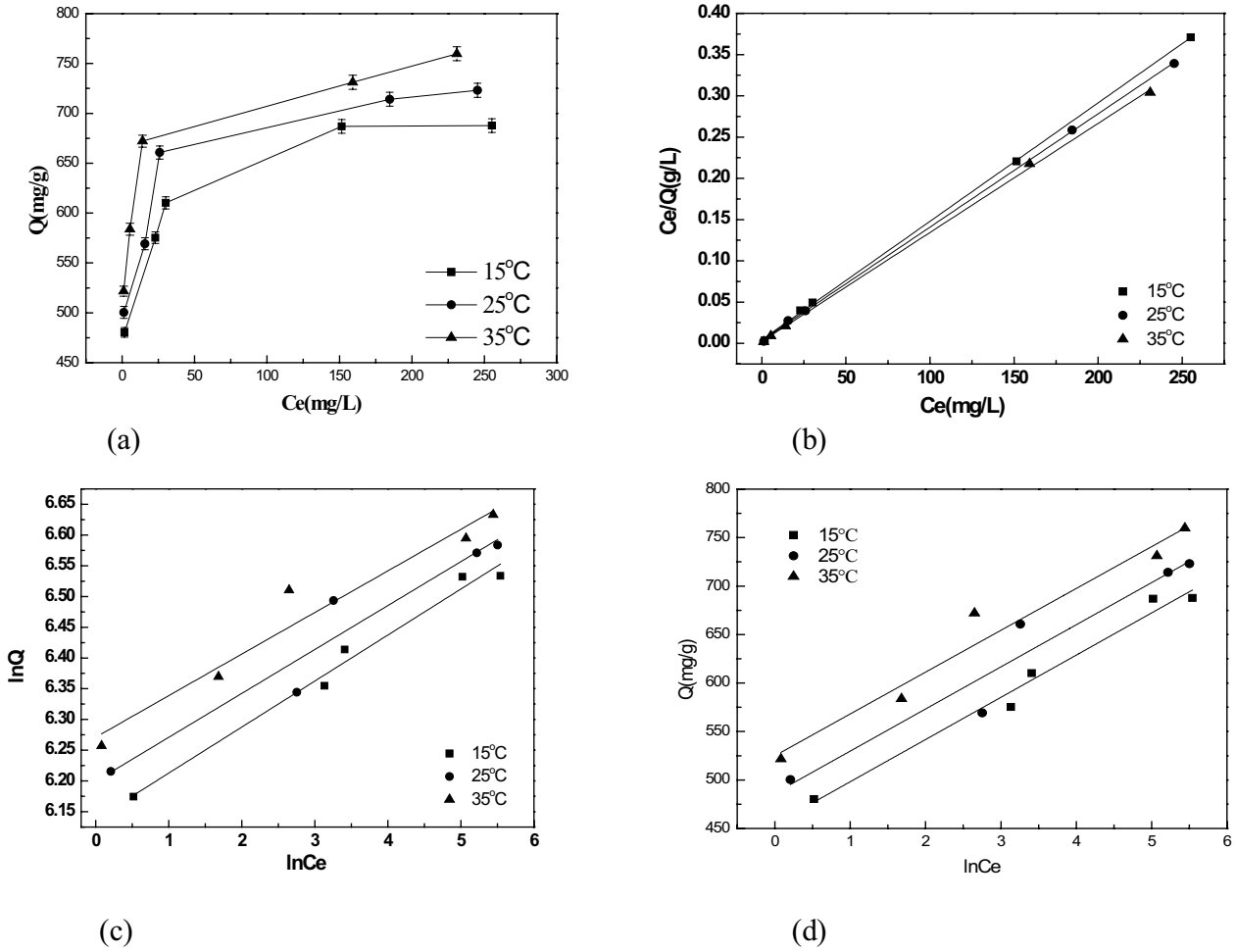

Fig. 5. Isotherm for the adsorption of Pb(II) on DPA-MWCNTs at different solution temperatures (a), Langmuir isotherm obtained by using the linear method for the adsorption of Pb(II) on DPA-MWCNTs at different solution temperatures (b), Freundlich isotherm obtained by using the linear method for the adsorption of Pb(II) on DPA-MWCNTs at different solution temperatures (c), and Temkin isotherm obtained by using linear method for the sorption of Pb(II) on DPA-MWCNTs at different solution temperatures (d).

(Figs. 5b and c). The Langmuir isotherm model [21], which interpreted homogeneous adsorption systems, can be written as:

$$\frac{C_e}{q_e} = \frac{C_e}{q} + \frac{1}{qK_L} \tag{12}$$

where q_e is the adsorption capacity, mg/g; C_e is the equilibrium concentration of Pb(II), mg/L; q is the saturated adsorption capacity, mg/g and K_L is the Langmuir adsorption constant, L/mg.

The Freundlich isotherm model [21], which assumes the multilayer adsorption on the heterogeneous adsorption sites, can be expressed as follows:

$$\ln q_e = \ln K_F + \frac{\ln C_e}{n} \tag{13}$$

where q_e is the adsorption capacity, mg/g; C_e is the equilibrium concentration of Pb(II), mg/L; n is Freundlich constant and K_F is the binding energy constant reflecting the affinity of the adsorbents to metal ions, mg/g.

The adsorption data were also correlated with the Temkin isotherm model [22] according to Eq. (14):

$$q_e = B_T \ln K_T + B_T \ln C_e \tag{14}$$

where q_e is the adsorption capacity, mg/g; C_e is the equilibrium concentration of Pb(II), mg/L; B_T and K_T are the Temkin constants representing the heat of adsorption and the maximum binding energy (L/g), respectively.

The isotherm parameters of Langmuir, Freundlich and Temkin for the adsorption of lead ions (Table 3) obtained using least square method showed that the regression coefficients R^2 obtained from Langmuir model were very close to 1 (0.9993–0.9998), suggesting that Langmuir model could well interpret the studied adsorption procedure. As shown in Table 3, Figs. 5c and d, the Freundlich isotherm and the Temkin isotherm are not consistent with the obtained experimental data as well as the Langmuir

Table 3
Isotherm parameters of the Langmuir model, the Freundlich model and the Temkin model for the adsorption of Pb(II) on DPA-MWCNTs

Adsorbent	T (°C)	Langmuir			Freundlich		
		q (mg/g)	K_L (L/mg)	R^2	K_F (mg/g)	n	R^2
DPA-MWCNTs	15	694.44	0.3258	0.9997	463.11	13.3618	0.9781
	25	729.93	0.3870	0.9998	492.53	13.9978	0.9134
	35	757.58	0.5946	0.9993	529.07	14.7842	0.9375

Adsorbent	T (°C)	Temkin		
		$B_T \ln K_T$	B_T	R^2
DPA-MWCNTs	15	454.6694	43.5331	0.98134
	25	486.3382	43.4439	0.93373
	35	524.9847	43.1398	0.96317

model, the experimental results of lead ions adsorption obtained at all temperatures have been found to fit well the Langmuir isotherm model. From the comparison of correlation coefficients, it can be concluded that the data were fitted better by Langmuir equation than by Freundlich equation and Temkin equation, indicating that the adsorption of DPA-MWCNTs for Pb(II) ion obeys the Langmuir adsorption isotherm, and the maximum adsorption capacity of DPA-MWCNTs at 35°C is 757.58 mg/g. The comparison of the obtained value in this work with the data presented in the literatures for other adsorbents [23–32] has showed that the adsorption capacity of DPA-MWCNTs is relatively high when compared with several other adsorbents, and DPA-MWCNTs could be an excellent adsorbent for lead removal considering the maximum adsorption capacity (Table S1), and the excellent adsorption capacity has made it a good promising candidate for Pb(II) removal. It is well known that the Langmuir isotherm suggests that the adsorption occurs in the monolayer way on the homogenous active sites, where the adsorption of each adsorbate molecule onto the surface had equal adsorption activation energy. The fact shows that the adsorption of this hybrid adsorbent is attributed to monolayer adsorption, it is also observed that the process is endothermic in nature because the value of q increases with the rise in temperature from 15°C to 35°C, which is in good agreement with the above-mentioned thermodynamic research result. Therefore, in the equilibrium state, the distribution of lead ions between the aqueous solution and diphosphonic acid modified-MWCNTs surface is a crucial factor that determines the maximum adsorption capacity of DPA-MWCNTs, and the lead ions adsorption by DPA-MWCNTs is attributed to monolayer adsorption.

The adsorption selectivity is also an indispensable factor for evaluating the properties of an adsorbent, by which the adsorbent can be used to adsorb some specific metal ions or to separate some specific metal ions from mixed metal ions solutions. In order to study the adsorption selectivity of DPA-MWCTNs for Pb(II), 20.0 mg of the prepared DPA-MWCTNs has been added into 20 mL of solutions (binary systems containing equal initial concentrations) and the mixture has been shaken for 12 h. Then the solutions are separated from the adsorbents and the concentrations of metal ions have been detected by atomic absorption spectrometer. In this study, the adsorption selectivity of DPA-MWCNTs to the target ion Pb(II) has been evaluated by the competitive adsorption with Hg(II)/Cu(II)/Ni(II)/Co(II)/Cr(III)/Cd(II) as co-ions. The experimental results display that DPA-MWCNTs have strong affinity for Pb(II) in the aqueous solutions, and they can exhibit 100% selectivity for Pb(II) ions in the presence of Cu(II), Ni(II), Co(II), Zn(II), Cr(III) and Cd(II), suggesting a higher adsorption efficiency of DPA-MWCNTs for Pb(II) over these other coexisting metal ions. The above-mentioned research results show that DPA-MWCNTs has preferential affinity for lead ions and is very favorable for the removal of lead ions, and the high adsorption capacity makes them good promising candidate for Pb(II) removal.

In order to make the lead adsorption process clear, furthermore, some analysis methods have been used to study the corresponding adsorption mechanism. FT-IR analysis is a useful technology in exploring the adsorption behaviors of metal ions on adsorbents. In order to further confirm the adsorption mechanism of DPA-MWCNTs for Pb(II), the changes of characteristic peaks in the adsorbent before and after adsorption have been shown in Fig. S1. The band at 2,913 cm^{-1} assigned to (P)–O–H stretching vibration before adsorption was weakened after adsorption; moreover, there was a reduction in the hydroxyl (O–H) stretching band at around 3,437 cm^{-1}, indicating that the coordination of the phosphonic acid with lead(II) ions on DPA-MWCNTs, which indicated on the chemical interactions between the adsorbent and the adsorbate. Energy spectrum of DPA-MWCNTs before (a) and after (b) Pb(II) adsorption. Some other peaks attributed to certain functional groups were shifted, signifying the feasible participation of the functional groups on the surface of DPA-MWCNTs. For example, the –P=O stretching at 1,165 cm^{-1} was shifted to 1,087 cm^{-1}, and the strength of peak was also enhanced. The results further confirmed the complexation of organophosphonic acid and lead ions during the heavy metals removal process. Fig. S2 has presented EDX of DPA-MWCNTs before (a) and after (b) Pb(II) adsorption, the spectrum of DPA-MWCNTs after lead ion adsorption displays the peaks for

P, O, C and Pb, and the weight percentage of Pb is 72.04%, which indicates that DPA-MWCNTs have gotten a lot of lead on the adsorbent. SEM images of DPA-MWCNTs (1) and Pb-DPA-MWCNTs (2) have been shown in Fig. S3, after Pb(II) adsorption, DPA-MWCNTs still keep the structures of nanotubes. It could be seen that these nanotubes are aligned randomly, which is a benefit to the heavy metal adsorption. The morphology of the samples before and after lead adsorption is similar, demonstrating that the samples have good mechanical stability and they had not obviously been changed during the whole adsorption process. The porous structure parameters of DPA-MWCNTs and Pb-DPA-MWCNTs derived from the basis of the nitrogen adsorption data have been obtained (Fig. S4). It could be seen that they exhibit type III isotherm with distinct hysteresis loops according to the IUPAC classification, which is representative of mesopores. The BET surface area, and average pore diameter calculated from BJH desorption DPA-MWCNTs are 67.67 m^2g^{-1} and 24.22 nm, respectively, and these open pores are very favorable for the adsorption conducted on the surface of DPA-MWCNTs. Those values of Pb-DPA-MWCNTs are 83.56 m^2g^{-1} and 19.72 nm, respectively. Therefore, the hydroxylated MWCNTs have special structures that can absorb metal ions from aqueous solutions; moreover, it can provide binding sites to form covalent bonding with DPA. The mutual effects of the unique structural characteristics of MWCNTs and the chelating functional groups of the diphosphonic acid have greatly enhanced the metal ion adsorption performance. The high adsorption capacity of DPA-MWCNTs for lead ions could be explained by the adsorption, the electrostatic attraction and the coordination interaction. However, the cost of this adsorbent material is high due to the use of carbon nanotubes. Our following work will strive to reduce the cost of such adsorbent materials by increasing the use life of the adsorbents, developing low-cost industrial-grade carbon nanotubes-based adsorbents and so on.

Moreover, the adsorption behavior of DPA-MWCNTs for the lead ions with low concentrations has been studied according to the study by Mirza and Ahmad [33] in the range of 10–100 mg/L; however, the adsorbent DPA-MWCNTs has very so strong adsorption ability for Pb(II) that % efficiency of Pb(II) removal showed 100% when the initial concentrations of lead ions were below 50 mg/L, then its corresponding maximum adsorption capacity could not be calculated. Therefore, the isotherm of Pb(II) on DPA-MWCNTs at different solution temperatures was studied in the range of initial concentration 50–100 mg/L, and Fig. S5a showed the isotherm for the adsorption of Pb(II) with low initial concentration on DPA-MWCNTs at different solution temperatures. Langmuir and Freundlich fitting were carried out (Figs. S5b and c), and it was found that the Freundlich fitting coefficient was greater than the Langmuir fitting coefficient at each temperature (Table S2), which was similar with the results in Mirza and Ahmad [33], and the results indicated that in the range of the initial lead concentrations of 50–100 mg/L, the experimental data were more consistent with the Freundlich fitting.

3.5. Recycling properties of DPA-MWCNTs

To evaluate the reusability of this prepared adsorbent, the related desorption experiments have been conducted to the lead ions loaded DPA-MWCNTs, that is, spent DPA-MWCNTs, are immersed in 0.1 mol/L nitric acid with different concentrations of thiourea at 25°C for 24 h to remove the lead ions and then neutralized and followed with a second round of lead ions adsorption testing. The results of elution in Fig. S6 show that the system of 0.1 mol/L nitric acid + 5.0% thiourea is very efficient, which could make lead ions almost completely eluted, and the relative elution rate is up to 89.76% during this process. After that, DPA-MWCNTs are washed with deionized water and ethanol, then dried and used further for adsorption studies. The adsorption and desorption cycles are repeated to study the reuse properties of DPA-MWCNTs. The results for lead ions adsorption using the regenerated DPA-MWCNTs are summarized in Table S3, it is clear that the lead ions uptake capacities decrease slowly in the successive uses. Only a little decrease of the adsorption efficiency is observed after three regenerations, the lead ions uptake capacities of DPA-MWCNTs retain 85.84%, which indicate that the functional diphosphonic acid groups on the surface of DPA-MWCNTs can be regenerated with only a little loss of functional activity in each cycle during the recycling process, its elution effect is still significant after three cycles, which further demonstrates the capability of DPA-MWCNTs for reuse.

3.6. Response surface methodology

In order to improve the adsorption capacities and the efficiency of the work, RSM has been utilized to indicate the parameters for an optimized adsorption process. The experimental design has been performed out by three chosen independent process variables at three levels (Table 4). It allows the user to gather large amounts of information from a small number of experiments, and also observe the effects of individual variables and their combinations of interactions on the response [33]. RSM has been applied to model the adsorption capacity of

Table 4
Coded levels for independent factors used in the experimental design

Factors	Symbol	Coded levels		
		–1	0	1
Initial pH	X_1	5.0	5.5	6.0
Adsorbent dosage/mg (DPA-MWCNTs)	X_2	5	10	15
Initial Pb(II) concentrations/mmol/L	X_3	1.5	2.0	2.5

DPA-MWCNTs for lead ions from stimulated wastewater with three reaction parameters, that is, initial pH, adsorbent dosage and initial Pb(II) concentration. The observed and predicted results of batch runs conducted in CCD experiments are tabulated in Table 5. Then, a series of 15 experimental runs defined by a CCD experiment for the optimization of adsorption conditions have been planned and carried out. The application of response surface methodology expressed in the following regression equation (Eq. (15)) is an empirical relationship between adsorption capacity (Y) and tested variables take in coded unit:

Table 5
Experimental design of 3-level 3-variable Box-Behnken design

No.	X_1	X_2	X_3	Adsorption capacities of DPA-MWCNTs /mmol/g	
				Experimental	Fitted value
1	1	1	0	2.69	2.6200
2	–1	0	–1	3.50	3.4925
3	–1	0	1	4.19	4.1775
4	–1	1	0	2.67	2.6200
5	0	0	0	3.64	3.6400
6	1	–1	0	3.05	3.1000
7	0	0	0	3.63	3.6400
8	1	0	–1	3.46	3.4725
9	0	–1	1	3.69	3.6325
10	0	–1	–1	3.72	3.6575
11	–1	–1	0	2.62	2.6900
12	0	0	0	3.65	3.6400
13	1	0	1	4.60	4.6075
14	0	1	–1	2.39	2.4475
15	0	1	1	4.23	4.2925

$$Y = 3.64 + 0.10X_1 - 0.14X_2 + 0.46X_3 - 0.23X_1^2 - 0.66X_2^2 + 0.52X_3^2 - 0.10X_1X_2 + 0.11X_1X_3 + 0.47X_2X_3 \quad (15)$$

where Y is the response (adsorption capacity), and X_1, X_2 and X_3 are the coded values of the main effects of initial pH, adsorbent dosage, and initial Pb(II) concentration, respectively. The coefficients for the model and the ANOVA are shown in Table 6. The significance of each coefficient was determined by t-values and p-values. The quadratic fitted equation (Eq. (15)) has been found to be statistically significant, as clearly seen from the value of model F-test (F = 108.85) with a low probability value of P, which demonstrates a high significance for the regression model. It is known that the larger the magnitude of the t-value and smaller the p-value, the more significant is the corresponding coefficient [33]. Therefore, the variable with the largest effect is initial lead ions concentration. Moreover, the interaction of DPA-MWCNTs dosage and initial Pb(II) concentration (X_2X_3) were highly significant, and both of the quadratic terms of adsorbent dosage (X_2^2) and initial lead ions concentration (X_3^2) are very

Table 6
Coefficients of the model and ANOVA[a]

Terms	Coefficients	Standard error	t-Start	p-value
Intercept	3.6400	0.04461	81.597	0.000
X_1	0.1025	0.02732	3.752	0.013
X_2	–0.1375	0.02732	–5.033	0.004
X_3	0.4550	0.02732	16.656	0.000
X_1X_1	–0.2263	0.04021	–5.627	0.002
X_2X_2	–0.6562	0.04021	–16.320	0.000
X_3X_3	0.5238	0.04021	13.025	0.000
X_1X_2	–0.1025	0.03863	–2.653	0.045
X_1X_3	0.1125	0.03863	2.912	0.033
X_2X_3	0.4675	0.03863	12.101	0.000

ANOVA

Source	Degrees of freedom	Sum of squares	Mean sum of squares	F	P
Regression	9	5.84872	0.649858	108.85	0.000
Linear	3	1.89150	0.630500	105.61	0.000
Square	3	2.99035	0.996783	166.97	0.000
Interaction	3	0.96687	0.322292	53.99	0.000
Residual error	5	0.02985	0.005970		
Lack of fit	3	0.02965	0.009883	98.83	0.010
Pure error	2	0.00020	0.000100		
Total	14	5.87857			

[a]Coefficient of determination (R^2) = 0.9949.

insignificant. The goodness of the fit of the model has also been checked by the multiple correlation coefficient. The value of the determination coefficient (R^2) is 0.9949, which indicates that the model is suitable to represent the real relationships among the selected reaction parameters, and the sample variation of 99.49% for the adsorption process is attributed to the independent variables and only 0.51% of the total variations has not been explained by the model, indicating that the obtained model was fitting the experimental results well. Moreover, the insignificant lack-of-fit test also means that the model is suitable to represent the experimental data using the designed experimental data.

The three-dimensional response surfaces corresponding to the obtained empirical equation (Eq. (15)) as a function of two independent variables, keeping the other constant at its central level has been displayed in Fig. 6, in which the adsorption capacities of DPA-MWCNTs over different combinations of independent variables have been visualized through three-dimensional view of response surface plots. The relationship between adsorbent dosage and initial pH was shown in Fig. 6a. It is true that the pH of aqueous solution is a highly influential adsorption variable, and it not only influences the ionization and the speciation of lead ions in aqueous solution but also strongly affects the electrostatic forces between lead cations and phosphonic acid-containing functional groups of the adsorbent DPA-MWCNTs surface. However, it is clear in Fig. 6a that the adsorbent dosage exerted stronger influence than the initial pH, which could also be deduced from the coefficients of factors in Eq. (15). It has been observed that the Pb(II) adsorption capacities increase at first, but decrease with further increasing DPA-MWCNTs dosage. Though increasing adsorbent dosage can be attributed to increased surface area and availability of more adsorption sites, higher DPA-MWCNTs dosage could result in aggregates of the functionalized adsorbent, and might cause interference between binding sites at higher DPA-MWCNTs dosage or insufficiency of lead ions in the solutions with respect to available binding sites. The effect of initial Pb(II) concentrations and initial pH on lead ions removal has been presented in Fig. 6b; it is found that when compared with the effect of pH, the initial lead ions concentration plays a greater role. As shown in Fig. 6c, a significant interaction has been found between initial Pb(II) concentration and adsorbent dosage (p = 0.000 and the absolute value of t-value is 12.101). According to the figure, it is obvious that the adsorption capacities increase with increasing the initial concentration of lead ions, which could be related to the increase in the number of collisions between lead ions and DPA-MWCNTs, as well as the increase in driving force of the concentration gradient, overcoming the mass transfer resistance [34]. Depending on the targeted

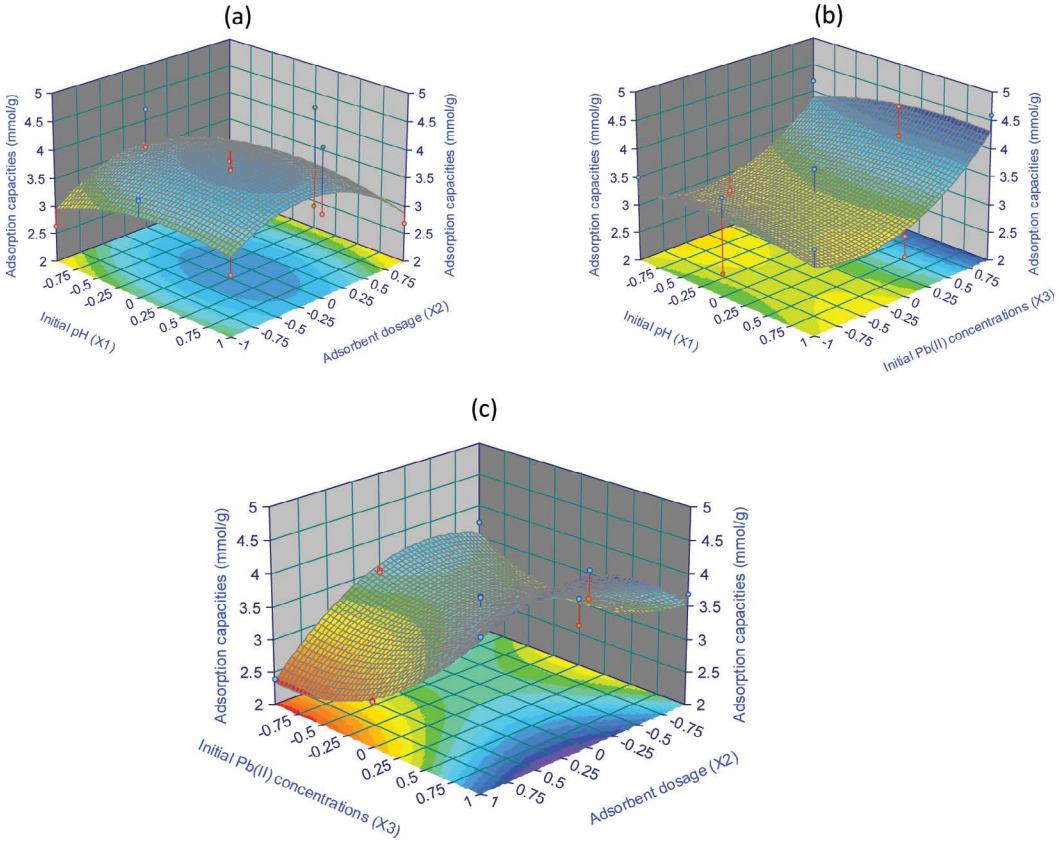

Fig. 6. Interaction and response surface of the process variables on the adsorption capacities for Pb(II) onto DPA-MWCNTs. (a) Surface plot of adsorption capacities for Pb(II) in term of adsorbent dosage and initial pH, (b) surface plot of adsorption capacities for Pb(II) in term of initial Pb(II) concentrations and initial pH, and (c) surface plot of adsorption capacities for Pb(II) in term of adsorbent dosage and initial Pb(II) concentrations.

application of DPA-MWCNTs, the desirable response might be adsorption capacity; the maximum predicted adsorption capacity for optimum adsorption variables could be obtained through point prediction method and response surface plots. The optimal conditions for lead adsorption using DPA-MWCNTs are X_1 = 5.71, X_2 = 11.09 mg, and X_3 = 2.5 mmol/L, that is, initial pH of 5.71, 11.09 mg/10.0 mL of DPA-MWCNTs dosage and the initial Pb(II) concentration of 2.5 mmol/L, and the theoretical maximum adsorption capacity was 4.70 mmol/g. To confirm the prediction by the model, three independent experiments for the lead adsorption over DPA-MWCNTs have been conducted under the established optimal conditions. The experimental adsorption capacity reached 4.65 ± 0.08 mmol/g, that is, close to the predicted value. At present, carbon nanotubes have been used to remove lead ions from aqueous solution, but their adsorption capacity is not very high (e.g., 147 mg/g [35]). In addition, we tried to modify diphosphonic acid functional groups on other solid matrix material (e.g., rice hulls), and it was found that the adsorption capacity of diphosphonic acid-modified rice hull was not very high (80.78 mg/g). So far, there is no literature reported to use diphosphonic acid modified carbon nanotubes to remove lead ions from aqueous solution, and the adsorption capacity of the modified material DPA-MWCNTs in this paper (764.42 mg/g) is much more than unmodified carbon nanotubes. Therefore, the novelty of this research work is both the assembly of a novel efficient adsorption material and the synergistic effect of carbon nanotubes and diphosphonic acid functional groups. The above-mentioned research results show that DPA-MWCNTs is very favorable for lead ions removal, and the excellent adsorption properties make them good promising candidate for the removal of Pb(II). In order to further promote the commercial viability of these adsorbents, the functionalization of low-cost industrial grade MWCNTs will be investigated in the future.

4. Conclusion

Because of speedily growing industrialization, many natural water resources have been polluted by toxic lead ions beyond its permission limits, and lead removal has become a global great concern in the recent years. In the present work, the feasibility of using diphosphonic acid modified multi-walled carbon nanotubes DPA-MWCNTs for adsorption of lead ions from wastewater has been investigated. The adsorption performance of DPA-MWCNTs has been evaluated using batch experiments, which includes adsorption kinetics, isotherm, thermodynamics and so on. The investigation indicates that the best interpretation for the experimental data could be given by the Langmuir isotherm equation, the maximum adsorption capacities of DPA-MWCNTs at 35°C is 757.58 mg/g. The adsorption kinetics of DPA-MWCNTs can be modeled by the pseudo-second-order rate equation successfully, and the adsorption thermodynamic parameters ΔG, ΔH and ΔS are –4,949.78 kJ mol^{-1}, 48.33 kJ mol^{-1}, and 172.02 J K^{-1} mol^{-1}, respectively. Furthermore, the optimal process conditions have been explored by RSM. The optimum values for maximum adsorption capacity could be obtained using a Box–Behnken center-united design with a minimum of experimental work. Under the optimal conditions, the predicted value of the adsorption capacity for lead ions has reached 4.65 ± 0.08 mmol/g. All these research work results present that the excellent features of DPA-MWCNTs with high efficiency for water purification and toxic lead ions removal may ensure their applicability and feasibility in the industrial scale.

Acknowledgments

This work has been supported by the National Natural Science Foundation of China (No. 51673090, 21806070, and 51102127), the Science and Technology Development Plan from Shandong Provincial Education Department (NO.J17KA006), and the Nature Science Foundation of Shandong Province (No. ZR2018PB017).

References

[1] M.E. Lee, J.H. Park, J.W. Chung, Comparison of the lead and copper adsorption capacities of plant source materials and their biochars, J. Environ. Manage., 236 (2019) 118–124.
[2] S.S. Fiyadh, M.A. AlSaadi, W.Z. Jaafar, M.K. AlOmar, S.S. Fayaed, N.S. Mohd, L.S. Hin, A. El-Shafie, Review on heavy metal adsorption processes by carbon nanotubes, J. Cleaner Prod., 230 (2019) 783–793.
[3] S. Debnath, U.C. Ghosh, Kinetics: isotherm and thermodynamics for Cr(III) and Cr(VI) adsorption from aqueous solutions by crystalline hydrous titanium oxide, J. Chem. Thermodyn., 40 (2008) 67–77.
[4] Y. Ding, D. Jing, H. Gong, L. Zhou, X. Yang, Biosorption of aquatic cadmium(II) by unmodified rice straw, Bioresour. Technol., 114 (2012) 20–25.
[5] T.S. Anirudhan, S.S. Sreekumari, Adsorptive removal of heavy metal ions from industrial effluents using activated carbon derived from waste coconut buttons, J. Environ. Sci., 23 (2011) 1989–1998.
[6] J. Hosseini, E. Nazarzadeh, D. Ajloo, Experimental and theoretical calculation investigation on effective adsorption of lead(II) onto poly(aniline-co-pyrrole) nanospheres, J. Mol. Liq., 296 (2019) 111789.
[7] Y. Jin, C. Zeng, Q. Lv, Y. Yu, Efficient adsorption of methylene blue and lead ions in aqueous solutions by 5-sulfosalicyclic acid modified lignin, Int. J. Biol. Macromol., 123 (2019) 50–58.
[8] W. Yang, Z. Wang, S. Song, J. Han, H. Chen, X. Wang, R. Sun, J. Cheng, Adsorption of copper(II) and lead(II) from seawater using hydrothermal biochar derived from *Enteromorpha*, Mar. Pollut. Bull., 149 (2019) 110586.
[9] K. Tomasz, K. Anna, C. Ryszard, Effective adsorption of lead ions using fly ash obtained in the novel circulating fluidized bed combustion technology, Microchem. J., 145 (2019) 1011–1025.
[10] S. Zhang, Q. Shi, C. Christodoulatos, X. Meng, Lead and cadmium adsorption by electrospun PVA/PAA nanofibers: batch, spectroscopic, and modeling study, Chemosphere, 233 (2019) 405–413
[11] A.H. El-Sheikh, F.S. Nofal, M.H. Shtaiwi, Adsorption and magnetic solid-phase extraction of cadmium and lead using magnetite modified with schiff bases, J. Environ. Chem. Eng., 7 (2019) 103229.
[12] S. Mohan, V. Kumar, D.K. Singh, S.H. Hasan, Effective removal of lead ions using graphene oxide-MgO nanohybrid from aqueous solution: isotherm, kinetic and thermodynamic modeling of adsorption, J. Environ. Chem. Eng., 5 (2017) 2259–2273.
[13] H. Wang, H. Shang, X. Sun, L. Hou, M. Wen, Y. Qiao, Preparation of thermo-sensitive surface ion-imprinted polymers based on multi-walled carbon nanotube composites for selective

adsorption of lead(II) ion, Colloids Surf. A, (in Press) https://doi.org/10.1016/j.colsurfa.2019.124139.
[14] S. Wang, W. Gong, X. Liu, Y. Yao, B. Gao, Q. Yue, Removal of lead(II) from aqueous solution by adsorption onto manganese oxide-coated carbon nanotubes, Sep. Purif. Technol., 58 (2007) 17–23.
[15] N.M. Mubarak, J.N. Sahu, E.C. Abdullah, N.S. Jayakumar, Removal of heavy metals from wastewater using carbon nanotubes, Sep. Purif. Methods, 43 (2014) 311–338.
[16] G. Mamba, X.Y. Mbianda, P.P. Govender, Phosphorylated multiwalled carbon nanotube-cyclodextrin polymer: synthesis, characterization and potential application in water purification, Carbohydr. Polym., 98 (2013) 470–476.
[17] Y. Tian, P. Yin, R. Qu, C. Wang, H. Zheng, Z. Yu, Removal of transition metal ions from aqueous solutions by adsorption using a novel hybrid material silica gel chemically modified by triethylenetetraminomethylenephosphonic acid, Chem. Eng. J., 162 (2010) 573–579.
[18] N.M. Bandaru, N. Reta, H. Dalal, A.V. Ellis, J. Shapter, N.H. Voelcker, Enhanced adsorption of mercury ions on thiol derivatized single wall carbon nanotubes, J. Hazard. Mater., 261 (2013) 534–541.
[19] K. Fujiwara, A. Ramesh, T. Maki, H. Hasegawa, K. Ueda, Adsorption of platinum (IV), palladium (II) and gold (III) from aqueous solutions onto L-lysine modified crosslinked chitosan resin, J. Hazard. Mater., 146 (2007) 39–50.
[20] T.S. Anirudhan, P.G. Radhakrishnan, Thermodynamics and kinetics of adsorption of Cu(II) from aqueous solutions onto a new cation exchanger derived from tamarind fruit shell, J. Chem. Thermodyn., 40 (2008) 702–709.
[21] A. Mehdinia, S. Heydari, A. Jabbari, Synthesis and characterization of reduced graphene oxide-Fe_3O_4@ polydopamine and application for adsorption of lead ions: isotherm and kinetic studies, Mater. Chem. Phys., 239 (2020) 121964.
[22] J. Kończyk, S. Żarska, W. Ciesielski, Adsorptive removal of Pb(II) ions from aqueous solutions by multi-walled carbon nanotubes functionalised by selenophosphoryl groups: kinetic, mechanism, and thermodynamic studies, Colloid Surf. A, 575 (2019) 271–282.
[23] R.A. Jacques, E.C. Lima, S.L.P. Dias, A.C. Mazzocato, F.A. Pavan, Yellow passion-fruit shell as biosorbent to remove Cr(III) and Pb(II) from aqueous solution, Sep. Purif. Technol., 57 (2007) 193–198.
[24] M.R. Awual, M.M. Hasan, A ligand based innovative composite material for selective lead(II) capturing from wastewater, J. Mol. Liq., 294 (2019) 111679.
[25] A.M. Hassan, W.A.W. Ibrahim, M.B. Bakar, M.M. Sanagi, Z.A. Sutirman, H.R. Nodeh, M.A. Mokhter, New effective 3-aminopropyltrimethoxysilane functionalized magnetic sporopollenin-based silica coated graphene oxide adsorbent for removal of Pb(II) from aqueous environment, J. Environ. Manage., 253 (2020) 109658.
[26] S. Tiwari, A. Hasan, L.M. Pandey, A novel bio-sorbent comprising encapsulated *Agrobacterium fabrum*(SLAJ731) and iron oxide nanoparticles for removal of crude oil co-contaminant, lead Pb(II), J. Environ. Chem. Eng., 5 (2017) 442–452.
[27] M. El-Sayeda, A.A. Nada, Polyethylenimi−functionalized amorphous carbon fabricated from oil palm leaves as a novel adsorbent for Cr(VI) and Pb(II) from aqueous solution, J. Water Process Eng., 16 (2017) 296–308.
[28] D. Afzali, M. Fayazi, Deposition of MnO_2 nanoparticles on the magnetic halloysite nanotubes by hydrothermal method for lead(II) removal from aqueous solutions, J. Taiwan Inst. Chem. Eng., 63 (2016) 421–429.
[29] M. Naushad, Z.A. ALOthman, M.R. Awual, M.M. Alam, G.E. Eldesoky, Adsorption kinetics, isotherms, and thermodynamic studies for the adsorption of Pb^{2+} and Hg^{2+} metal ions from aqueous medium using Ti(IV) iodovanadate cation exchanger, Ionics, 21 (2015) 2237–2245.
[30] A.A.H. Faisal, S.F.A. Al-Wakelb, H.A. Assib, L.A. Najia, M. Naushad, Waterworks sludge-filter sand permeable reactive barrier for removal of toxic lead ions from contaminated groundwater, J. Water Process Eng., 33 (2020) 101112.
[31] Q. Zeng, Y. Huang, L. Huang, L. Hu, W. Sun, H. Zhong, Z. He, High adsorption capacity and super selectivity for Pb(II) by a novel adsorbent: nano humboldtine/almandine composite prepared from natural almandine, Chemosphere, 253 (2020) 126650.
[32] F. An, R. Wu, M. Li, T. Hu, J. Gao, Z. Yuan, Adsorption of heavy metal ions by iminodiacetic acid functionalized D301 resin: kinetics, isotherms and thermodynamics, React. Funct. Polym., 118 (2017) 42–50.
[33] A. Dean, D. Voss, D. Draguljić, Design and Analysis of Experiments, Springer International Publishing, Cham, 2017, pp. 565–614.
[34] R. Bardestani, C. Roy, S. aliaguine, The effect of biochar mild air oxidation on the optimization of lead(II) adsorption from wastewater, J. Environ. Manage., 240 (2019) 404–420.
[35] K. Yang, Z. Lou, R. Fu, J. Zhou, J. Xu, S.A. Baig, X. Xu, Multiwalled carbon nanotubes incorporated with or without amino groups for aqueous Pb(II) removal: comparison and mechanism study, J. Mol. Liq., 260 (2018) 149–158.

Supporting information

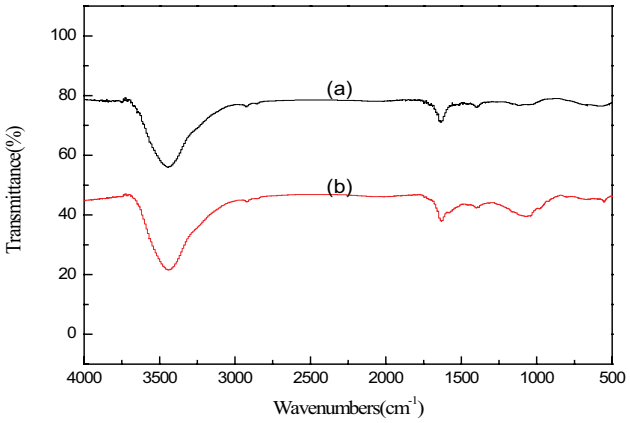

Fig. S1. FT-IR spectra of the adsorbent DPA-MWCNTs before (a) and after (b) Pb(II) adsorption.

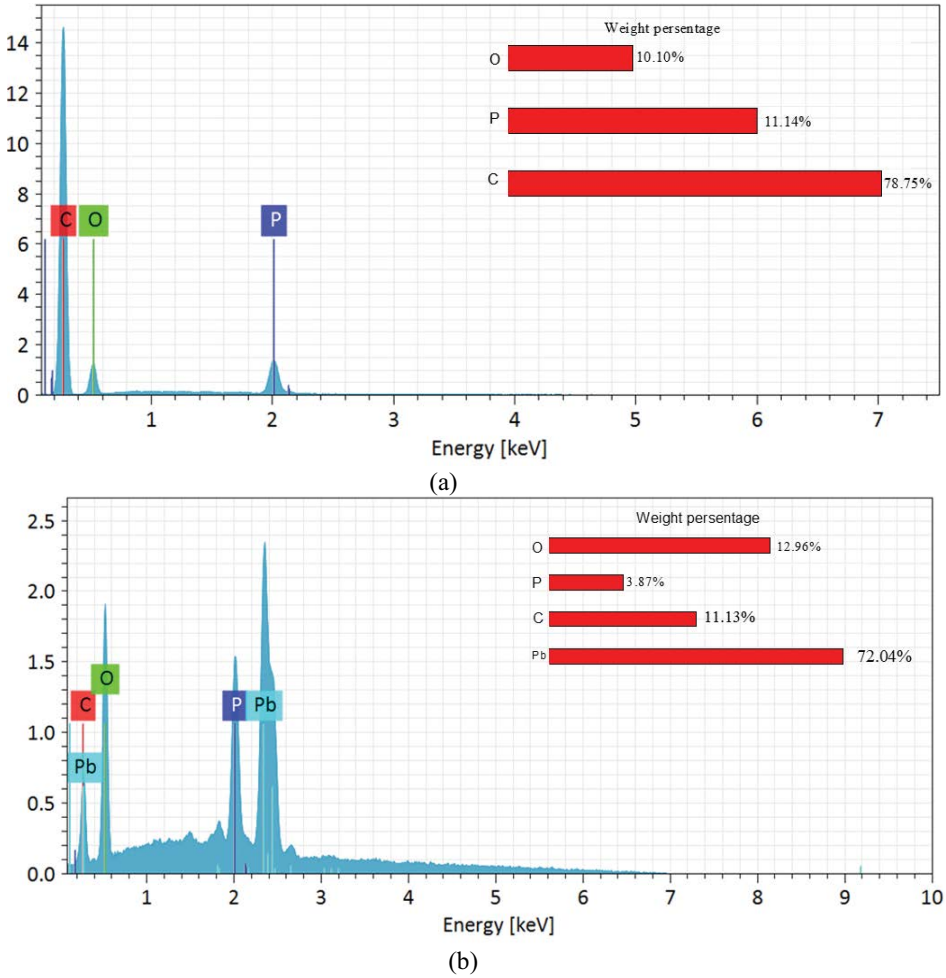

Fig. S2. EDX of DPA-MWCNTs before (a) and after (b) Pb(II) adsorption.

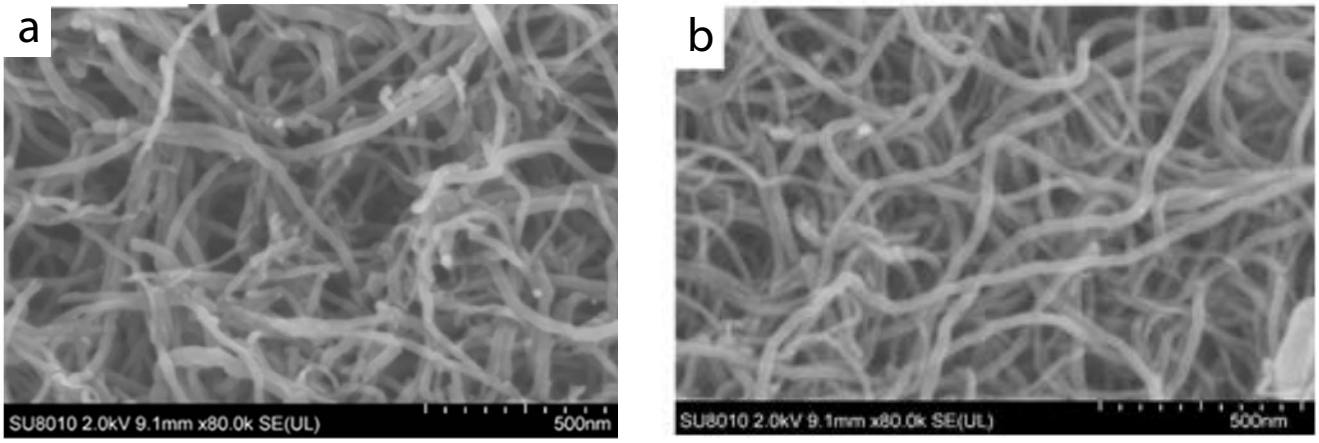

Fig. S3. SEM images of DPA-MWCNTs before (a) and after (b) Pb(II) adsorption.

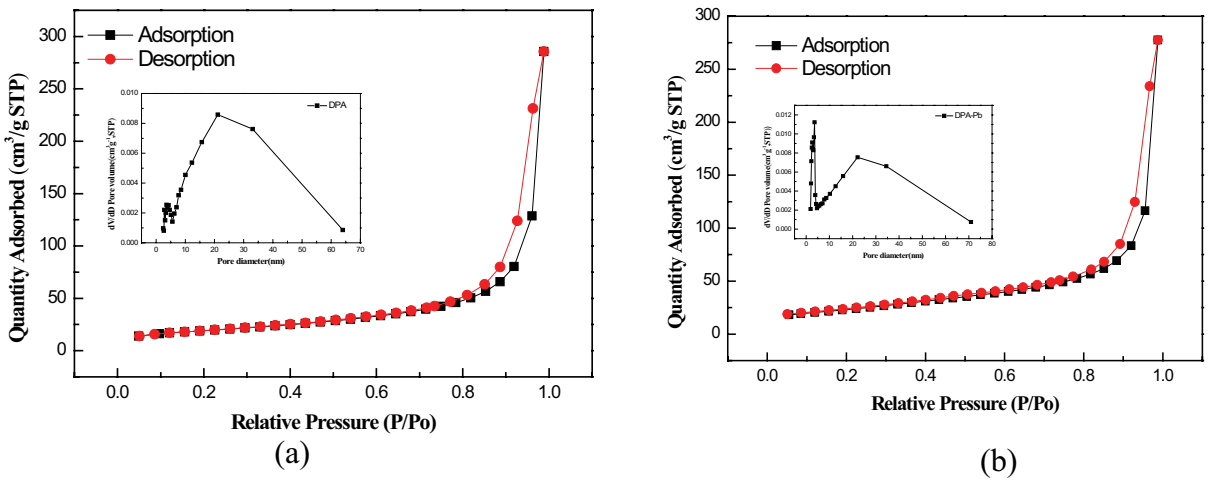

Fig. S4. N_2 adsorption–desorption isotherms and pore size distribution (inset figures) of DPA-MWCNTs before (a) and after (b) Pb(II) adsorption.

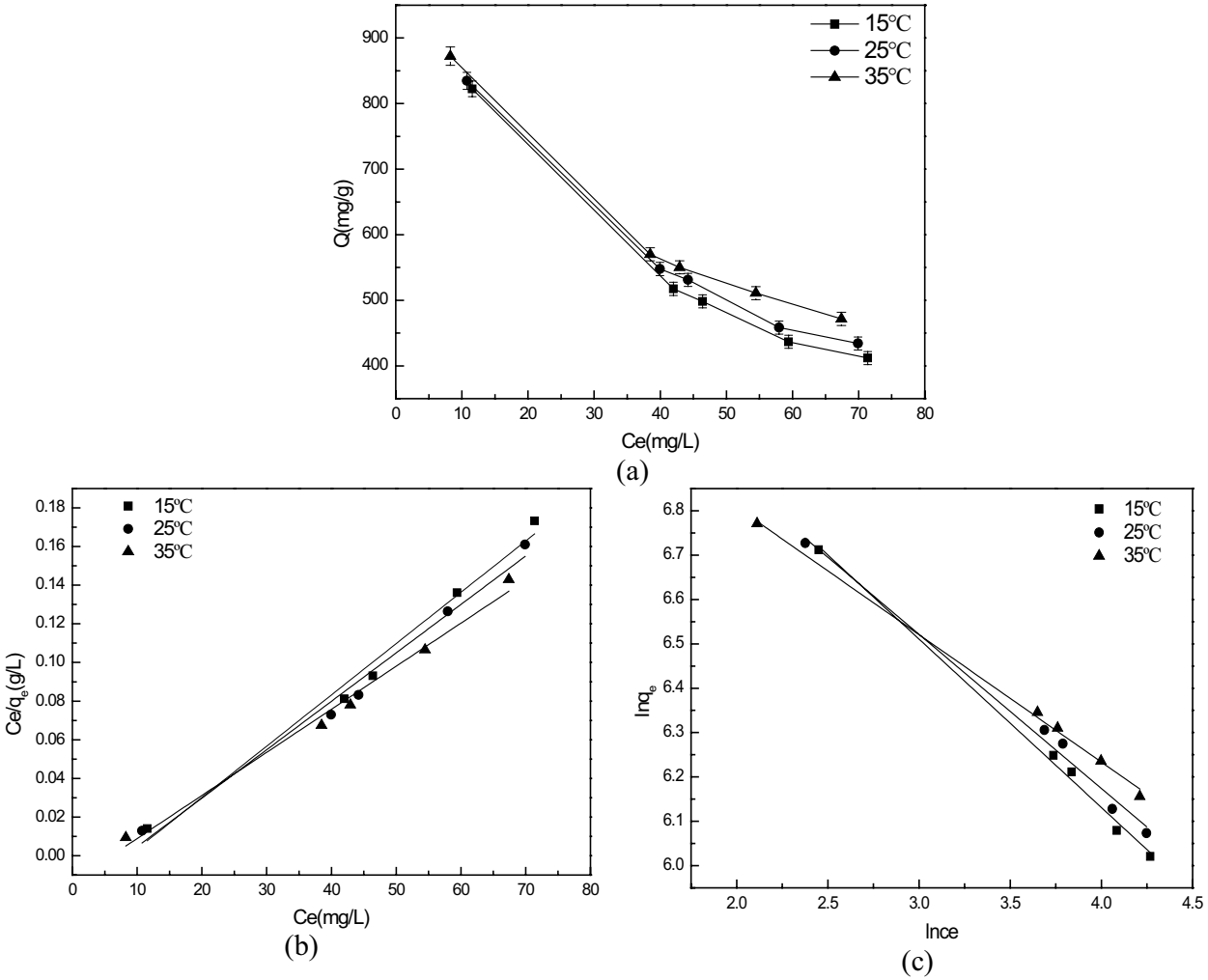

Fig. S5. Isotherm for the adsorption of Pb(II) with low initial concentrations on DPA-MWCNTs at different solution temperatures (a), Langmuir isotherm obtained by using the linear method for the adsorption of Pb(II) on DPA-MWCNTs at different solution temperatures (b), Freundlich isotherm obtained by using the linear method for the adsorption of Pb(II) on DPA-MWCNTs at different solution temperatures (c).

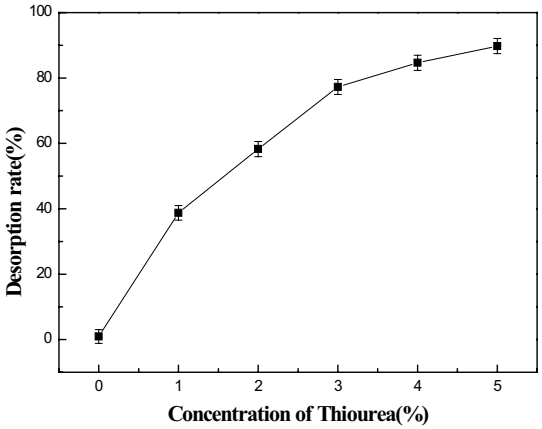

Fig. S6. Effects of different concentrations of thiourea on the desorption rate of DPA-MWCNTs for lead ions.

Table S1
Adsorption capacities of different adsorbents for lead ions

Adsorbents	Q_e (mg/g)	Literatures
Yellow passion-fruit shell	151.6	[23]
MBHB	214.15	[24]
GO@SiO_2-MSp@SiO_2NH_2	323.5	[25]
WBMNPs	197.02	[26]
ACTF-PEI	143.0	[27]
MHNTs@MnO_2	59.9	[28]
TIV	18.8	[29]
Waterworks sludge	20.41	[30]
NHLA composite	574.71	[31]
IDA-functionalized D301	618.93	[32]
DPA-MWCNTs	757.58	This work

Table S2
Isotherm parameters of the Langmuir model and the Freundlich model for the adsorption of Pb(II) with low initial concentrations on DPA-MWCNTs

Adsorbent	T (°C)	Langmuir			Freundlich		
		q (mg/g)	K_L (L/mg)	R^2	K_F (mg/g)	n	R^2
DPA-MWCNTs	15	377.36	0.3258	0.9824	2,099.63	2.63373	0.9947
	25	398.42	0.3870	0.9811	1,928.10	2.87688	0.9883
	35	454.56	0.5946	0.9863	1,608.30	3.47971	0.9970

Table S3
Regeneration properties of DPA-MWCNTs

Regeneration times		DPA-MWCNTs
1	q (mmol/g)	1.96
	Desorption rate (%)	89.76
2	q (mmol/g)	1.94
	Desorption rate (%)	87.48
3	q (mmol/g)	1.87
	Desorption rate (%)	85.84